P1.61 Impact of the mass-accomodation coefficient on cirrus

Robert W. Carver and Jerry Y. Harrington*
Department of Meteorology, Pennsylvania State University, University Park, PA

1. Introduction

Recent laboratory research done by Magee (2006) suggests that the value of α_d, in typical cirrus environments is much smaller than values published in the literature. This is important because the effective vapor diffusivity at the crystal's surface, D_v^*, depends on α_d. For small crystals with a length, a,

$$D_v^* = \frac{D_v}{\frac{a}{a+\Delta_v} + \frac{D_v}{a\alpha_d}\sqrt{\frac{2\pi M_w}{\mathcal{R}T_a}}}. \quad (1)$$

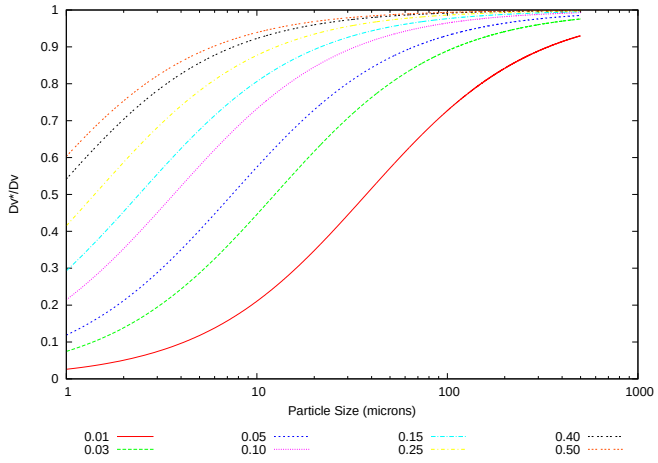

Figure 1: Plot of D_v^*/D_v as a function of crystal size

Figure 1 is a plot of D_v^*/D_v for several different values of α_d. It is immediately apparent that $D_v^* < D_v$ for small crystal sizes and low values of α_d. So if α_d is truly small for cirrus environments, then it is apparent that the crystal will grow following the modified vapor diffusivity instead of the bulk vapor diffusivity.

This has considerable implications for ice clouds as noted by Gierens et al. (2003). First, let us consider an environment supersaturated with respect to ice. Since $D_v^* < D_v$, mass growth rates calculated using the modified vapor diffusivty will be smaller than those rates calculated with D_v. This is important because bulk microphysics parameterizations use D_v, which means growth rates of small ice crystals are likely too large.

2. Impact of Diffusivity

To examine the potential effects of small α_d on cirrus, we will use RAMS to study the 16 July 2002 CRYSTAL-FACE case study using the methodologies presented in Carver et al. (2003), and the new sedimentation parameterization in Carver and Harrington (2005).

2a. *Effects of α_d Parameterization*

Even though RAMS has two ice categories, pristine ice and snow, it would only be appropriate to include the effects of α_d on pristine ice. This is because pristine ice in RAMS includes only very small crystals, if the characteristic diameter, D_N of the pristine ice distribution exceeds 125 microns, part of the pristine ice mixing ratio and number concentration are added to the snow category to reduce D_N. The valid range of D_N ranges from 125 to 10000 microns, and since Fig. 1 shows that the effects of D_V^* would be minor for large crystals, it would not be appropriate to parameterize the effects of α_d for snow.

Recall the vapor growth equation for a single crystal

*Corresponding author address: J. Harrington, Dept. of Meteorology, Penn State University, University Park, PA 16802. email: harring@mail.meteo.psu.edu

with a size, D,

$$\frac{dm}{dt} = 4\pi D D_v \left(\rho_{vi} - \rho_{v\infty}\right) \tag{2}$$

It then follows that the change in mixing ratio, $\frac{dM}{dt}$ is then given by,

$$\frac{dM}{dt} = \int \frac{dm}{dt} n(D) dD \tag{3}$$

So we can then express $\frac{dM}{dt}$ as,

$$\frac{dM}{dt} = \int 4\pi D D_v \left(\rho_{vi} - \rho_{v\infty}\right) n(D) dD \tag{4}$$

If D_v is constant as typically assumed for bulk ice microphysics models, then

$$\frac{dM}{dt} = 4\pi D_v \left(\rho_{vi} - \rho_{v\infty}\right) \int 4\pi D D_v \left(\rho_{vi} - \rho_{v\infty}\right) n(D) dD \tag{5}$$

However, D_v^* varies with D, so it would seem that we would be required to integrate D_v^* for every distribution. There is another possibility, Klemp and Wilhelmson (1978) use a average of the ventilation coefficient in the evaporation equation, instead of integrating it for each distribution. This suggests that we can use a diameter-weighted average of D_v^* in the following fashion,

$$\frac{dM}{dt} = 4\pi \langle D_v^* \rangle \left(\rho_{vi} - \rho_{v\infty}\right) \int 4\pi D D_v \left(\rho_{vi} - \rho_{v\infty}\right) n(D) dD \tag{6}$$

where,

$$\langle D_v^*(D_N) \rangle = \int_0^{0.1m} D_v^* n(D) dD \tag{7}$$

For a preliminary evaluation of the effects of including the vapor accommodation coefficient, we use (6) and (7) for as the vapor growth parameterization for pristine ice. For computational efficiency, we compute values of $\langle D_v^*(D_N \rangle$ for $1\mu m \leq D_N \leq 125\mu m$, the limits for pristine ice, and calculate a fit to these values using the following form,

$$\langle D_v^*(D_N) \rangle = a D_N^b + c D_N^d + e \tag{8}$$

Tests show that this set of parameterizations accurately represent the behavior of D_v^* integrated for each distribution.

Figure 2 is a plot of IWC after 4 hours using the normal D_v, and Fig. 3 is a similar plot using the $\langle D_v^*(D_N) \rangle$

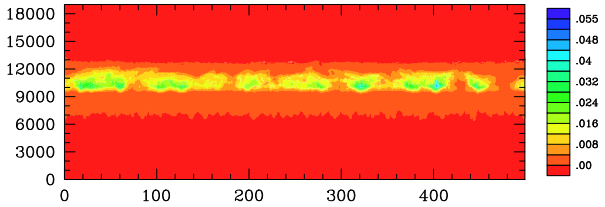

Figure 2: Plot of IWC at t=4 hours using standard D_v

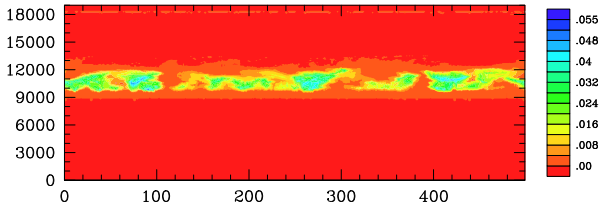

Figure 3: Plot of IWC at t=4 hours using $\langle D_v^* \rangle$

parameterization with $\alpha_d = 0.005$. It is clear that including the effects of α_d leads to significant shifts in the total amount of condensate and cloud structure. To better understand how α_d effects cloud dynamics and morphology, a series of simulations were produced using a range of values of α_d from the value of 0.005 measured by Magee (2006) to the theoretical maximum of 1.0.

2b. *Radiative Properties*

Figure 4 plots the maximum absolute values and altitude of the radiative heating and cooling for the cloud. The maximum values were chosen since they typically represent the longwave warming at cloud base and the shortwave cooling at cloud top that drive the buoyancy circulations of a layer cloud. This plot shows that as α_d approaches the measured value, the intensity of radiative heating and cooling increases and the altitude of the maxima increases as well. The increase in radiative flux divergence is likely responsible for lifting the cloud compared to the baseline simulation. Figure 4 suggests that changes in effective radius are responsible for the changes in radiative flux since the effective radius decreases sharply with α_d.

2c. *Microphysical Properties*

Figure 6 shows that the diameter of the mode of the mass distribution for pristine ice crystals does not change significantly with α_d, but that the diameter for snow crystals does decrease rapidly. This is likely why the effective radius decreases rapidly with α_d. Figure 7 also shows that the maximum mixing ratio and number concentration of pristine ice grows rapidly with decreasing α_v, while the mixing ratio and number concentration for snow shrinks rapidly. This indicates that during the cloud's lifecycle, the amount of water vapor that contributes to the growth of large crystals is much less than the amount of vapor consumed by the nucleation and growth of large numbers of small crystals for simulations using appropriate values of α_d.

These results are somewhat consistent with those of Gierens et al. (2003), suggesting that our parameterization for a bulk microphysics model is producing the same physics as their bin microphysics model but our results do not show any significant change for $\alpha_d = 0.1$ as their results do. This may be a consequence of having to neglect the effects of α_d for snow, or it could be a consequence of our case being a subtropical anvil simulation and the other case being a simulation of midlatitude cirrus.

Given such shifts in crystal diameter, it follows that there should be changes in the maximum sedimentation fall speed. Figure 9 shows that the fall speed for the maximum pristine mixing ratio does not change significantly with α_d, but the fall speed for snow crystals does decrease sharply. This is significant since the mass flux from sedimentation plays an important role in determing cloud lifetime (Starr and Cox 1985; Boehm et al. 1999).

2d. *Cloud Dynamics*

Figure 9 shows that as α_d decreases, the maximum value and maximum standard deviation of the updraft speeds increase relative to the baseline. The standard deviation of the updraft speed is a rough proxy of the structure of the updrafts at a given vertical level. Low standard deviations imply a smooth, nearly uniform updraft covering a large area. Large standard deviations suggest updrafts with rapidly varying velocities across a vertical level, which implies a turbulent structure. This means that simulations using appropriate values of α_d will have stronger updrafts and more structure than simulations that do not account for the mass accommodation coefficient. A similar analysis (not shown) of the cloud downdrafts suggests that they behave like the updrafts

2e. *Cloud Lifetime*

Given all of these changes in cloud properties, one would expect there to be differences in the modeled cloud life time based on the choice of α_d. An increase in radiative flux divergence would create stronger vertical motions in the cloud, increasing cloud lifetime as suggested by (Boehm et al. 1999). A decrease in average particle side would lead to reduced mass flux out of the cloud due to sedimentation, leading to increase cloud longevity as suggested by (Starr and Cox 1985).

Figure 10 is a plot of cloud lifetime, which is defined as the amount of time for the average optical depth of the cloud to fall below 1.0. The sharp rise in cloud lifetime for small α_d agrees with our predictions. It is immediately obvious that the modeled cloud lifetime is very sensitive for to changes in α_d when it is small, but that is insensitive to changes when $\alpha_d > 0.1$. However, our results disagree with Gierens et al. (2003), in that we do not see significant changes for $\alpha_d = 0.1$

3. Conclusions

There are several conclusions to be drawn from this research. First, the behavior of simulated cirrus decks is sensitive to the value of α_d. By controlling the amount and size of small crystals, α_d can significanly alter cloud dynamics, microphysics, and radiation leading to major shifts in cloud morphology and lifetime, whic are important for understanding the radiative forcing of cirrus . Using cloud lifetime as a metric, it appears that simulations using $\alpha_d > 0.1$ are not signficantly different than simulations that use the bulk vapor diffusion coefficient. If α_d is truly smaller than previous research has suggested, then the applicability to the real world of modeling studies that use large α_d or neglect its effects must be questioned.

4. Acknowledgments

This research has been funded as part of NASA CRYSTAL FACE and by DOE ARM under Grant no. DF-FG02-05ER64058.

References

Boehm, M. T., J. Verlinde, and T. P. Ackerman, 1999: On the maintenance of high tropical cirrus. *Journal of Geophysical Research (Atmospheres)*, **104**, 24423–24434, doi:10.1029/1999JD900798.

Carver, R. W., J. Harrington, and J. Verlinde, 2003: Simulations of the July 16 and 21 CRYSTAL-FACE Cirrus Cases Using a Cloud-Resolving Model Forced by a Mesoscale Model. *AGU Fall Meeting Abstracts*, H8+.

Carver, R. W. and J. Y. Harrington, 2005: Simulations of the July 16 and 21 CRYSTAL-FACE Cirrus Cases Using a Cloud-Resolving Model With an Improved Sedimentation Parameterization. *AGU Spring Meeting Abstracts*, C3+.

Gierens, K. M., M. Monier, and J.-F. Gayet, 2003: The deposition coefficient and its role for cirrus clouds. *Journal of Geophysical Research (Atmospheres)*, **108**, 10–+, doi:10.1029/2001JD001558.

Klemp, J. B. and R. B. Wilhelmson, 1978: The Simulation of Three-Dimensional Convective Storm Dynamics. *Journal of Atmospheric Sciences*, **35**, 1070–1096.

Magee, N., 2006: *A Laboratory Investigation of Vapor-Grown Ice Crystals at Low Atmospheric Temperatures*. Ph.D. thesis, Department of Meteorology, Pennsylvania State University.

Starr, D. O. and S. K. Cox, 1985: Cirrus Clouds. Part I: A Cirrus Cloud Model. *Journal of Atmospheric Sciences*, **42**, 2663–2681.

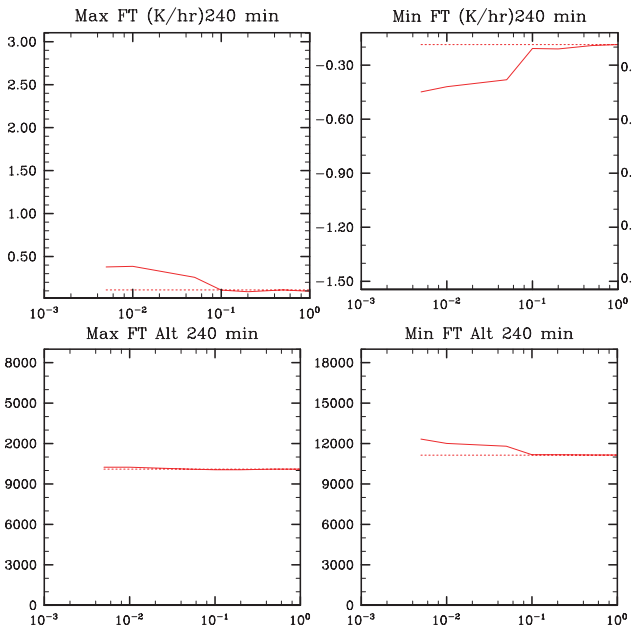

Figure 4: Plot of altitude and value of maximum/minimum radiative cooling at t=4 hours. The solid line is for simulations using $\langle D_v^* \rangle$, and the dashed line represents the value for a simulation using D_v.

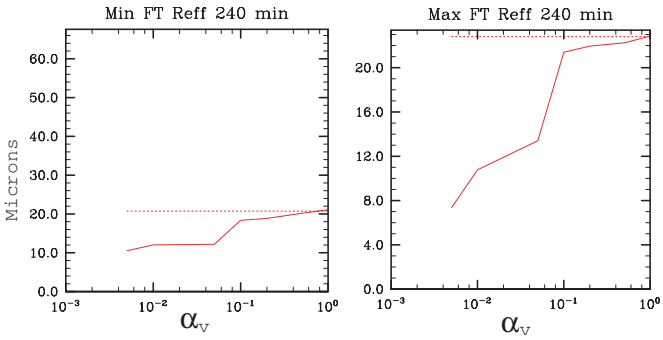

Figure 5: Plot of effective radius for location of maximum/minimum radiative cooling. Same style as 4.

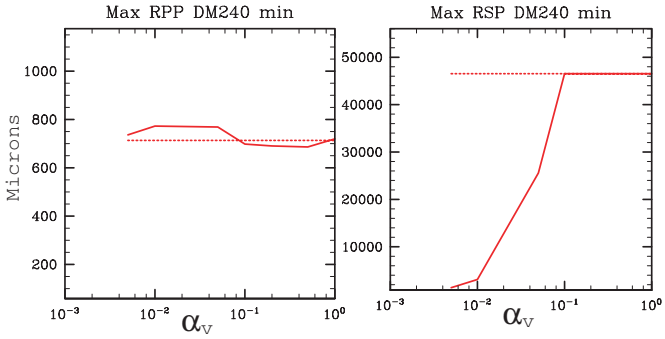

Figure 6: Plot of the diameter of the mode of the mass distribution for the maximum pristine/snow mixing ratios. Same style as 4.

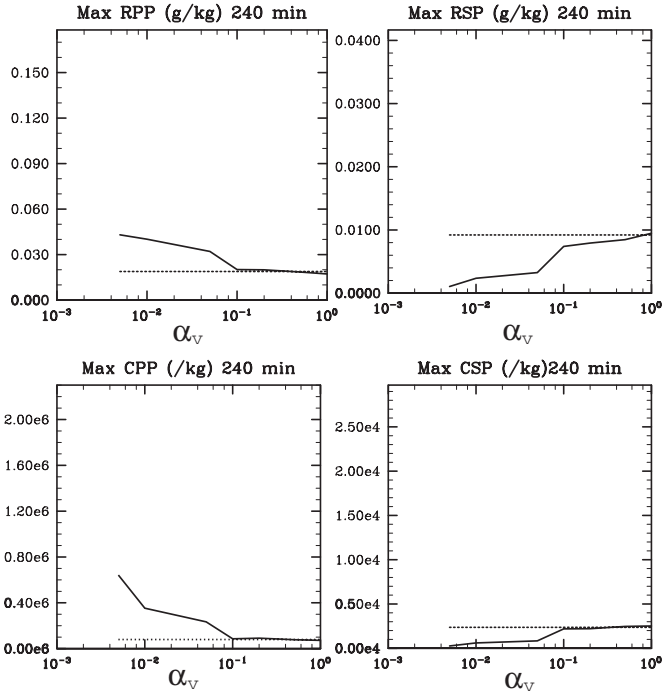

Figure 7: Plot of maximum pristine/snow mixing ratio and maximum number concentration at t=4 hours. Same style as 4.

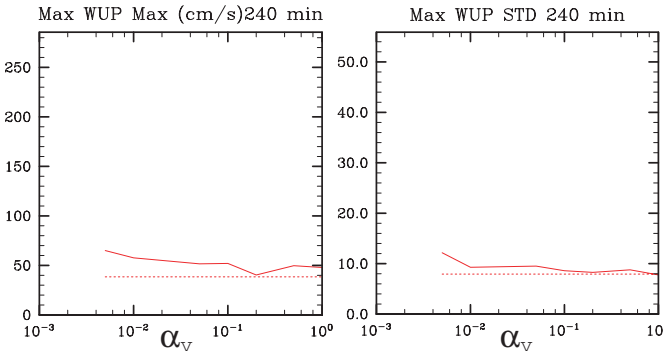

Figure 9: Plot of maximum value/standard deviation of updraft velocity. Same style as 4.

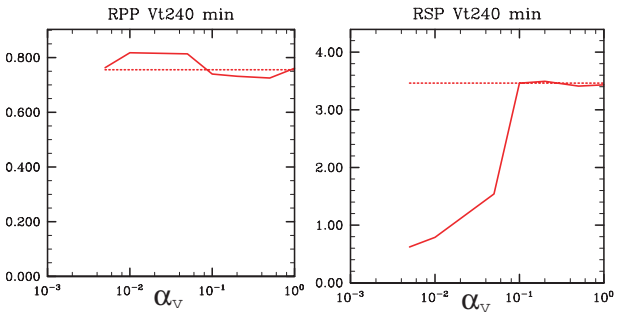

Figure 8: Plot of maximum terminal velocity for pristine/snow. Same style as 4.

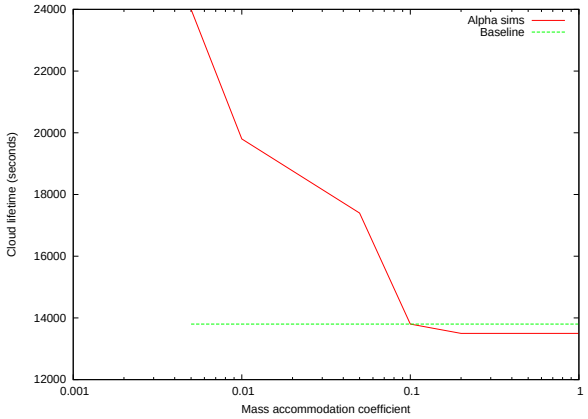

Figure 10: Plot of cloud lifetime